Staircase effect in field-induced metamagnetic transitions in La0×9Ce0×1Fe12B6

L.V.B. Diop, O. Isnard

Staircase effect in field-induced metamagnetic transitions in $La_{0.9}Ce_{0.1}Fe_{12}B_6$

L.V.B. Diop[1†] and O. Isnard[2]

[1]*Université de Lorraine, CNRS, IJL, F-54000 Nancy, France*

[2] *Université Grenoble Alpes, CNRS, Institut NEEL, 25 rue des martyrs, F-38042 Grenoble, France*

We report on peculiar magnetic-field-induced metamagnetic transitions in the antiferromagnetic itinerant-electron compound $La_{0.9}Ce_{0.1}Fe_{12}B_6$. Below 8 K, the first magnetization curves display multiple steep jumps generating a staircase-like shape. Whereas the magnetization of $La_{0.9}Ce_{0.1}Fe_{12}B_6$ varies smoothly with the external applied magnetic field at $T \geq 8$ K. We further show that this staircase effect is extremely sensitive to the thermomagnetic history of the sample.

1. Introduction

Recently, unconventional and discontinuous metamagnetic phase transitions were reported in $LaFe_{12}B_6$ system [1-4]. This peculiar multistep behavior is featured by extremely sharp magnetization steps followed by plateaus leading to an unusual and unique avalanche-like magnetization process. The itinerant-electron metamagnetic system $LaFe_{12}B_6$ occupies a special place among rare-earth iron-rich intermetallic compounds; it exhibits uncommon magnetic behavior and many intriguing physical properties. An amplitude-modulated antiferromagnetic structure described by a magnetic propagation vector **k** = (¼, ¼, ¼) and especially weak Fe magnetic moment of about 0.43 μ_B in the magnetically ordered ground state were revealed by neutron powder diffraction studies [1]. $LaFe_{12}B_6$ presents extraordinary low Néel temperature T_N = 36 K for an Fe-rich intermetallic phase, a multicritical point in the complex magnetic phase diagram [1], both inverse and normal magnetocaloric phenomenon [5], colossal spontaneous magnetization steps [3], and large magnetovolume effects [6]. These singular properties not only tendered the development of experiments under extreme conditions and theoretical models for a deeper understanding of the fascinating physics underlying the striking behavior of this compound [6-10], but also highlighted the potential interest of $LaFe_{12}B_6$ system in future low-temperature energy technologies. The ternary compound $LaFe_{12}B_6$ constitutes an exceptional playground for materials physics owing to the extreme sensitivity of its physical properties to reasonably weak external pressure [6] and chemical substitution that yields the effect of "chemical pressure" [4].

† leopold.diop@univ-lorraine.fr

Within the $RT_{12}B_6$ family (where R is a rare-earth atom and T stands for a 3d transition metal element Co or Fe) the RCo$_{12}$B$_6$ intermetallics are stable along the whole rare-earth series, whereas LaFe$_{12}$B$_6$ is the sole stable Fe-based compound of the 1:12:6 ternary system [9-11]. Even though NdFe$_{12}$B$_6$ alloy was the first Fe-based member of the $RT_{12}B_6$ ternary system to be identified, it is not stable [12]. At room temperature, the $RT_{12}B_6$ intermetallic phases adopt the rhombohedral SrNi$_{12}$B$_6$-type crystal structure with $R\bar{3}m$ space group [13-15]. In the unit-cell, there are two inequivalent positions for T atoms (18g and 18h). The R and B atoms reside on the *3a* and 18h Wyckoff sites, respectively. LaFe$_{12}$B$_6$ compound is unique within the $RT_{12}B_6$ family exhibiting an antiferromagnetic ground state with an ordering temperature much smaller than the Curie temperature of the Co-based RCo$_{12}$B$_6$ ferro- (R =Y, La-Sm) or ferri- (R = Gd-Tm) magnets (T_C =134 - 162 K) [11]. The Néel temperature of LaFe$_{12}$B$_6$ is an order of magnitude smaller when compared to the magnetic transition temperature of any rare-earth iron-rich binary alloy. Extraordinary magnetotransport properties have been most recently reported in RCo$_{12}$B$_6$ intermetallics with R = Y, Gd and Ho [16].

The present paper is a continuation of Refs. 4,19,20 and concerns the influence of thermomagnetic prehistory on the avalanche-like behavior of the magnetization. In this work, we examined by magnetization isotherms various aspects of the step-like metamagnetic transitions: minor hysteresis loops, sample dependence, reproducibility after thermal cycling, field cooling effect.

2. Experiments

The La$_{0.9}$Ce$_{0.1}$Fe$_{12}$B$_6$ polycrystalline compound was synthetized by arc-melting the mixture of high purity components (better than 99.9%) under a protective argon gas atmosphere. To purify the argon atmosphere inside the arc-melter, a Ti piece was melted in an adjacent recess of the water cooled copper hearth prior to the melting of the constituting elements. To ensure compositional homogeneity, the alloy was melted several times with the button being turned over after each re-melting. The so-obtained ingot was wrapped in Ta foil, sealed in an evacuated fused quartz tube and subsequently annealed at 1173 K for 3 weeks. The analysis of the phase purity and the room temperature crystallographic structure was performed by standard x-ray powder diffraction using a Siemens D5000 powder diffractometer in reflection mode with the Bragg–Brentano geometry and Co-Kα radiation ($\lambda_{K\alpha1}$ = 1.78897 Å and $\lambda_{K\alpha2}$ = 1.79285 Å). Isothermal magnetization curves were recorded, in applied fields of up to 10.5 T, on a powder sample using an extraction-type magnetometer. A detailed description of the magnetometer can be found in Ref. [17].

3. Results and discussion

In Fig. 1 we compare the magnetization isotherms of $LaFe_{12}B_6$ and $La_{0.9}Ce_{0.1}Fe_{12}B_6$ intermetallics. The compounds exhibit a magnetic-field-induced metamagnetic transition between the AFM and FM phases. Ce for La substitution leads to a pronounced diminution of both the critical field and the hysteresis width of the AFM-FM metamagnetic phase transformation. It is immediately apparent from a visual inspection of the reverse branch that there are big differences between $LaFe_{12}B_6$ and $La_{0.9}Ce_{0.1}Fe_{12}B_6$. In the Ce-containing alloy, the decreasing-field leg displays no transitions. As regards the parent compound $LaFe_{12}B_6$, the metamagnetic process is observed not only in the virgin magnetization curve (first magnetization curve), but in the envelope curve as well. Ce for La substitution induces both electronic and structural changes and therefore an alteration of the magnetic behavior under applied field. It is worth to notice that the lattice parameters of the $La_{1-x}Ce_xFe_{12}B_6$ series of compounds decrease with the Ce concentration. Such a reduction in cell dimensions is attributed to the smaller atomic size of Ce atoms compared to that of La atoms. The partial substitution of Ce for La in this system produces the effect of "chemical pressure" on the crystal lattice.

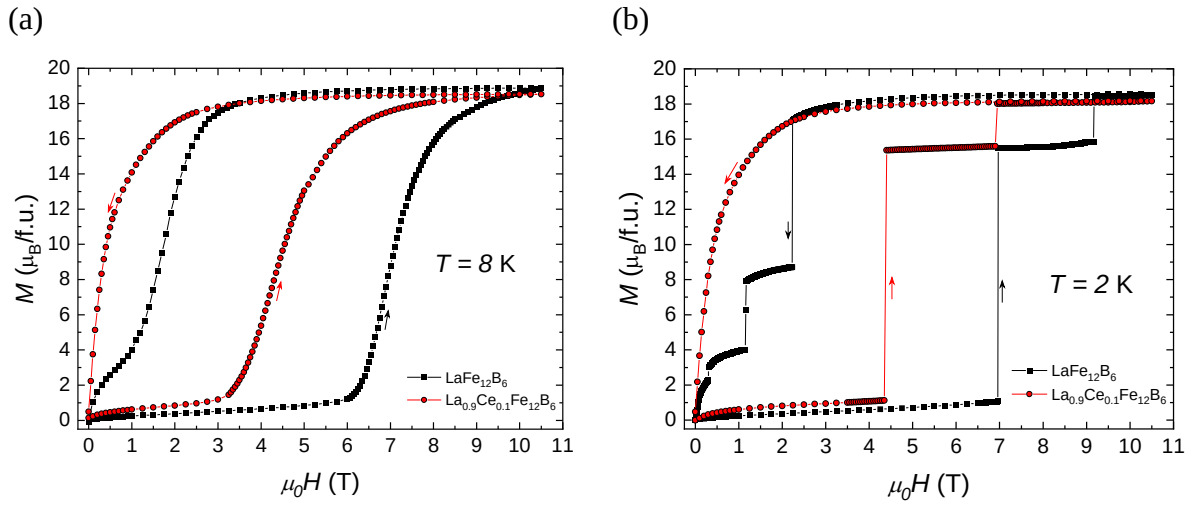

Fig. 1. Magnetization isotherms of $LaFe_{12}B_6$ (squares) and $La_{0.9}Ce_{0.1}Fe_{12}B_6$ (circles) compounds at (a) 8 K, and (b) 2 K.

The magnetization isotherms of the thermally demagnetized $La_{0.9}Ce_{0.1}Fe_{12}B_6$ at temperatures ranging between 2 and 8 K are illustrated in Fig. 2. Below 8 K, the virgin curves display two abrupt jumps followed by plateaus; generating a staircase-like metamagnetic process. These avalanche-like (or step-like) transitions result from conversion of fraction of the compound from the antiferromagnetic (AFM) ground state into the field-induced ferromagnetic (FM) state. The first magnetization plateau is associated with a magnetically heterogenous state,

i.e., a mixture of the AFM and FM phases (phase separated into AFM and FM domains). The saturation moment of the fully FM polarized state is estimated to be 18.22 μ_B/f.u. at 2 K. The subsequent decreasing-field scan shows no jumps neither metamagnetic transitions and exhibits a standard ferromagnetic behavior. This indicates that $La_{0.9}Ce_{0.1}Fe_{12}B_6$ remains in the forced FM state after the applied field is brought back to zero. The AFM-FM magnetic phase transformation is fully irreversible in this temperature region. The critical fields of the step transitions observed during the first application of the magnetic field increase as the temperature is lowered. One can also remark that the height of the plateau following the first magnetization jump diminishes with increasing temperature. In other words, the percentage of $La_{0.9}Ce_{0.1}Fe_{12}B_6$ transformed into FM phase during the first transition decreases upon heating. The sharpness of the magnetic-field-induced step-like transitions is reduced with increasing temperature and vanishing at 8 K where the metamagnetic process becomes continuous. Another salient feature in the 8 K isothermal magnetization curve is the remarkably large magnetic field hysteresis with a width of ≈ 4.1 T, which is consistent with the first-order character of the magnetic transformation.

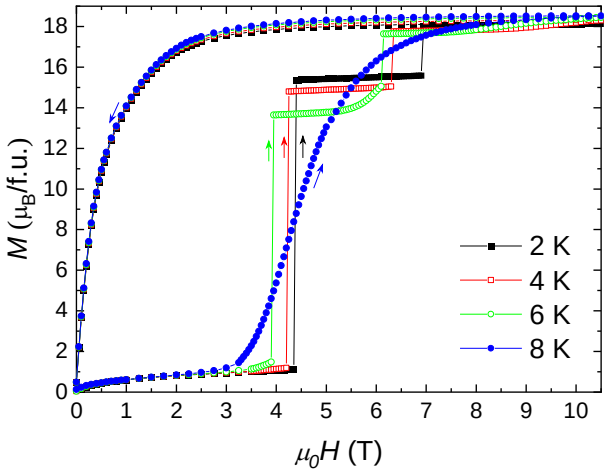

Fig. 2. Magnetization isotherms measured on $La_{0.9}Ce_{0.1}Fe_{12}B_6$ powder at temperature of 2, 4, 6 and 8 K.

We exemplify in Fig. 3 minor (up to 6 T) and complete (up to 10.5 T) hysteresis loops measured at 2 K. In both loops, it is noteworthy that the entire virgin curve (path 1) lies outside of the subsequent hysteresis envelope. During the first jump, a large amount, ~85%, of the sample volume is converted into a FM state, and ~15% remains in the initial AFM phase. The magnetization curve recorded when increasing the applied field after reversing the current direction to the superconducting magnet (path 3 in Fig. 3) is symmetrical to the demagnetization

path of the first quadrant. Both magnetization curves, obtained when rising the magnetic field from -6 to 6 T (−10.5 to 10.5 T) and when varying the field from 6 to -6 T (10.5 to -10.5 T), are practically superimposed. Once formed, the field-driven FM component is stable and $La_{0.9}Ce_{0.1}Fe_{12}B_6$ behaves as a soft ferromagnetic material with no remanent magnzetization and no coercivity. To restore the initial AFM ground state, it is necessary to warm up the sample above the ferromagnetic ordering temperature and subsequently cooled it down in zero magnetic field.

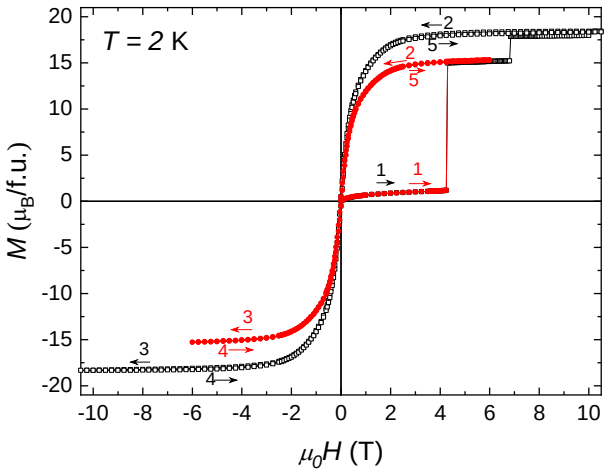

Fig. 3. Hysteresis loops of $La_{0.9}Ce_{0.1}Fe_{12}B_6$ powder sample at 2 K. The arrows indicate the field directions in which measurements have been performed.

The reproducibility of the ultrasharp multistep magnetization process was investigated. To explore more profoundly this point, repeated thermal cycling "300 K → 2 K → 300 K" in the absence of applied magnetic field was carried out and the magnetization isotherm was recorded each time at 2 K. The results of five runs are reported in Fig. 4. As it can be clearly seen from Fig. 4, the linear parts observed between 0.8 and 4.2 T in the ascending-field branch are identical. This demonstrates that the compound was entirely demagnetized between the cycles. The stepwise behavior is well reproducible. However, the height of the first plateau and the critical fields associated with the sudden jumps differ only slightly from one run to another. The reproducibility of the staircase effect was also investigated on six virgin specimen taken from the same batch (see Fig. 5). Each sample presents two discrete steps and very small variations are detected from sample to sample. In all case the saturation magnetization amounts to 18.22 μ_B/f.u. These experimental results attest to the good homogeneity of this series of polycrystalline samples.

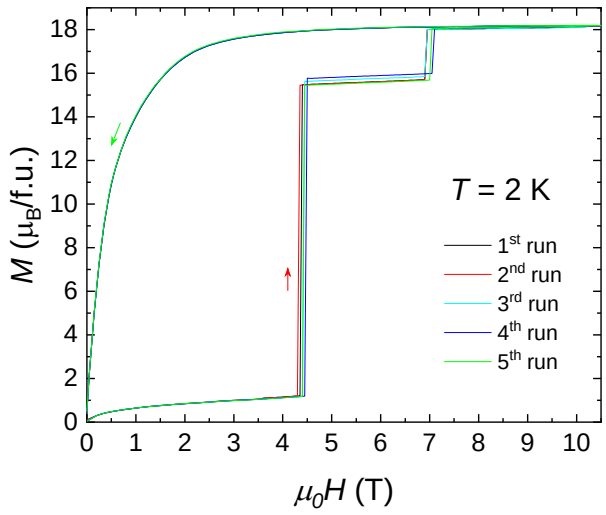

Fig. 4. Five magnetization isotherms at 2 K recorded successively for the same $La_{0.9}Ce_{0.1}Fe_{12}B_6$ sample. Each curve was recorded after a zero-field cooling from room temperature in order to restore the virgin AFM ground state.

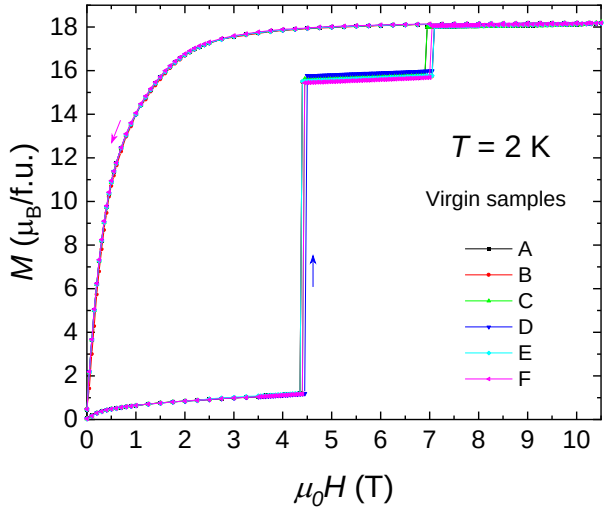

Fig. 5. Magnetization isotherms at 2 K for six virgin $La_{0.9}Ce_{0.1}Fe_{12}B_6$ samples coming from the same batch.

We have also examined the influence of the magnetic field strength applied during the cooling process on the magnetization. For such investigations, the intermetallic compound was cooled in the presence of a magnetic field ($\mu_0 H > 0$) from high temperatures (paramagnetic region) down to 2 K. After the temperature of 2 K is stabilized, the cooling field was removed, and subsequently isothermal magnetization curve was recorded (Fig. 6a). This magnetic field cooling process increases considerably the low-field magnetization owing to the growth of the FM phase proportion in the sample to the detriment of the AFM component. Field cooling shifts the sharp magnetization jumps towards higher magnetic fields. The critical fields (Fig. 6b) at which the step transitions occur are completely mastered by the residual FM phase

concentration. Cooling in an adequately high external field transforms the alloy into a fully FM polarized state, suppressing the sudden jumps. The thermomagnetic history affects strongly the staircase behavior found in the itinerant-electron metamagnetic compound $La_{0.9}Ce_{0.1}Fe_{12}B_6$. With respect to the reference compound $LaFe_{12}B_6$, field cooling decreases the critical fields of the step-like metamagnetic transitions [18] in contrast to what is observed for $La_{0.9}Ce_{0.1}Fe_{12}B_6$.

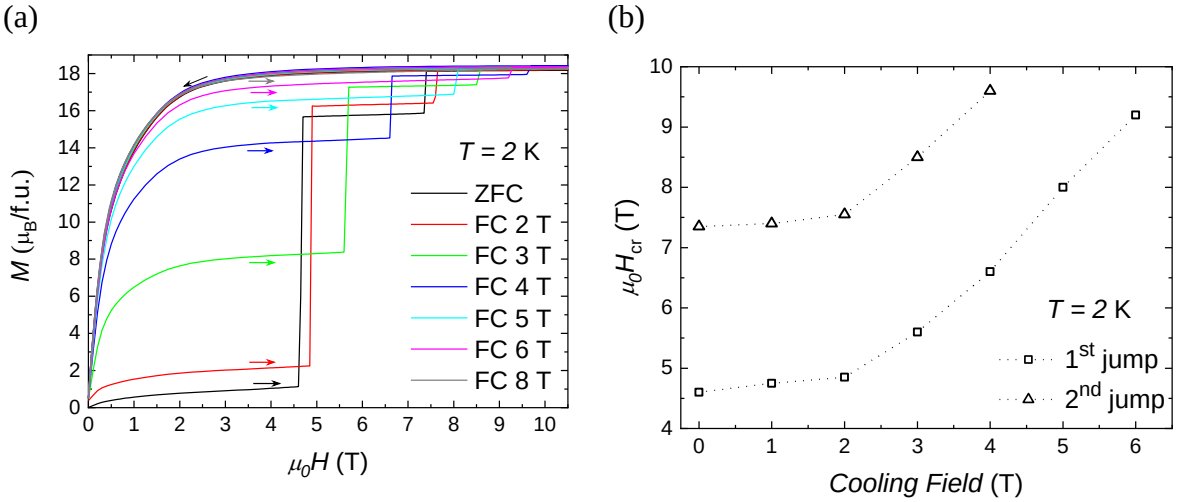

Fig. 6. (a) Magnetization isotherms of $La_{0.9}Ce_{0.1}Fe_{12}B_6$ compound at 2 K taken after cooling the sample in different magnetic fields from room temperature; (b) cooling field dependence of the critical field $\mu_0 H_{cr}$.

4. Summary

In summary we have performed a thorough experimental investigation of the staircase effect in the intermetallic compound $La_{0.9}Ce_{0.1}Fe_{12}B_6$ exhibiting an AFM ground state. This AFM order can be transformed into a FM state via a field-driven first-order metamagnetic phase transformation accompanied by a huge magnetic field hysteresis. In the very low temperature regime (T < 8 K), the metamagnetic process is discontinuous manifesting itself by a series of irreversible large sudden jumps in the virgin magnetization curves. The staircase behavior is found to be very sensitive to thermomagnetic cycling of the system.

References

[1] L. V. B. Diop, O. Isnard, and J. Rodríguez-Carvajal, Phys. Rev. B **93**, 014440 (2016).

[2] S. Fujieda, K. Fukamichi, and S. Suzuki, J. Magn. Magn. Mater. **421**, 403 (2017).

[3] L. V. B. Diop, and O. Isnard, Appl. Phys. Lett. **108**, 132401 (2016).

[4] L. V. B. Diop, and O. Isnard, Phys. Rev. B **97**, 014436 (2018).

[5] L. V. B. Diop, and O. Isnard, J. Appl. Phys. **119**, 213904 (2016).

[6] L. V. B. Diop, O. Isnard, Z. Arnold, J.P. Itié, J. Kastil, and J. Kamarad, Solid State Comm. **252**, 29 (2017).

[7] G. I. Miletic, and Z. Blazina, J. Magn. Magn. Mater. **323**, 2340 (2011).

[8] G. I. Miletic, and Z. Blazina, J. Alloys Compd. **430**, 9 (2007).

[9] M. Rosenberg, T. Sinnemann, M. Mittag, and K. H. J. Buschow, J. Alloys Compd. **182**, 145 (1992).

[10] Q. A. Li, C. H. de Groot, F. R. de Boer, and K. H. J. Buschow, J. Alloys Compd. **256**, 82 (1997).

[11] M. Mittag, M. Rosenberg, and K.H.J. Buschow, J. Magn. Magn. Mater. **82**, 109 (1989).

[12] K. H. J. Buschow, D. B. de Mooij, and H.M. van Noort, J. Less-Common Met. **125**, 135 (1986).

[13] K. Niihara, and S. Yajima, Chem. Lett. **1**, 875 (1972).

[14] Yu. B. Kuz'ma, G.V. Chernyak, and N.F. Chaban, Dopov. Akad. Nauk. Ukr. RSR Ser. A **12**, 80 (1981).

[15] W. Jung, and D. Quentmeier, Z. Kristallogr. **151**, 121 (1980).

[16] F. Mesquita, S. G. Magalhaes, P. Pureur, L.V.B. Diop, and O. Isnard, Phys. Rev. B **101**, 224414 (2020).

[17] A. Barlet, J. C. Genna, and P. Lethuillier, Cryogenic **31**, 801 (1991).

[18] L. V. B. Diop, and O. Isnard, J. Alloys Compd. **688**, 953 (2016).

[19] L.V.B. Diop, and O. Isnard, J. Appl. Phys. **129**, 243902 (2021).

[20] L.V.B. Diop, and O. Isnard, Eur. Phys. J. Plus **136**, 840 (2021).